Carrier-envelope-phase stabilized terawatt class laser at 1 kHz with a wavelength tunable option

Benjamin Langdon,[1,2] Jonathan Garlick,[1] Xiaoming Ren,[3] Derrek J. Wilson,[3] Adam M. Summers,[3] Stefan Zigo,[3] Matthias F. Kling,[3,4] Shuting Lei,[5] Christopher G. Elles,[6] Eric Wells,[7] Erwin D. Poliakoff,[8] Kevin D. Carnes,[3] Vinod Kumarappan,[3] Itzik Ben-Itzhak,[3] and Carlos A. Trallero-Herrero[3,*]

[1]*Kapteyn-Murnane Laboratories Inc., 1855 S 57th Ct, Boulder, Colorado 80301, USA*
[2]*Crunch Technologies, 3765 Birchwood Dr. #56, Boulder, Colorado 80304, USA*
[3]*J. R. Macdonald Lab., Kansas State University, 116 Cardwell Hall, Manhattan, Kansas 66506, USA*
[4]*Physics Department, Ludwig-Maximilians-Universität, Am Coulombwall 1, 85748 Garching, Germany*
[5]*Industrial and Manufacturing Systems Engineering, Kansas State University, Manhattan, Kansas 66506, USA*
[6]*Department of Chemistry, University of Kansas, Lawrence, Kansas 66045, USA*
[7]*Department of Physics, Augustana College, Sioux Falls, South Dakota 57197, USA*
[8]*Department of Chemistry, Louisiana State University, Baton Rouge, Louisiana 70803, USA*
[*]*trallero@phys.ksu.edu*

Abstract:
We demonstrate a chirped-pulse-amplified Ti:Sapphire laser system operating at 1 kHz, with 20 mJ pulse energy, 26 femtosecond pulse duration (0.77 terawatt), and excellent long term carrier-envelope-phase (CEP) stability. A new vibrational damping technique is implemented to significantly reduce vibrational noise on both the laser stretcher and compressor, thus enabling a single-shot CEP noise value of 250 mrad RMS over 1 hour and 300 mrad RMS over 9 hours. This is, to the best of our knowledge, the best long term CEP noise ever reported for any terawatt class laser. This laser is also used to pump a white-light-seeded optical parametric amplifier, producing 6 mJ of total energy in the signal and idler with 18 mJ of pumping energy. Due to preservation of the CEP in the white-light generated signal and passive CEP stability in the idler, this laser system promises synthesized laser pulses spanning multi-octaves of bandwidth at an unprecedented energy scale.

OCIS codes: (320.7090) Ultrafast lasers; (140.3280) Laser amplifiers; (120.5050) Phase measurement; (140.4050) Mode-locked lasers; (190.4975) Parametric processes.

References and links

1. F. Krausz and M. Ivanov, "Attosecond physics," Rev. Mod. Phys. **81**, 163–234 (2009).
2. D. Strickland and G. Mourou, "Compression of amplified chirped optical pulses," Opt. Commun. **55**, 447–449 (1985).
3. M. Nisoli, S. D. Silvestri, and O. Svelto, "Generation of high energy 10 fs pulses by a new pulse compression technique," Appl. Phys. Lett. **68**, 2793–2795 (1996).

#231111 - $15.00 USD Received 29 Dec 2014; accepted 2 Feb 2015; published 12 Feb 2015

4. C. P. Hauri, W. Kornelis, F. W. Helbing, A. Heinrich, A. Couairon, A. Mysyrowicz, J. Biegert, and U. Keller, "Generation of intense, carrier-envelope phase-locked few-cycle laser pulses through filamentation," Appl. Phys. B. **79**, 673–677 (2004).
5. C. P. J. Barty, C. L. Gordon, and B. E. Lemoff, "Multiterawatt 30-fs ti: sapphire laser system," Opt. Lett. **19**, 1442–1444 (1994).
6. M. D. Perry, D. Pennington, B. C. Stuart, G. Tietbohl, J. A. Britten, C. Brown, S. Herman, B. Golick, M. Kartz, J. Miller, H. T. Powell, M. Vergino, and V. Yanovsky, "Petawatt laser pulses," Opt. Lett **24**, 160–162 (1999).
7. H.-S. Chan, Z.-M. Hsieh, W.-H. Liang, A. H. Kung, C.-K. Lee, C.-J. Lai, R.-P. Pan, and L.-H. Peng, "Synthesis and measurement of ultrafast waveforms from five discrete optical harmonics," Science **331**, 1165 (2011).
8. A. Wirth, M. T. Hassan, I. Grguraš, J. Gagnon, A. Moulet, T. T. Luu, S. Pabst, R. Santra, Z. A. Alahmed, A. M. Azzeer, V. S. Yakovlev, V. Pervak, F. Krausz, and E. Goulielmakis, "Synthesized light transients," Science **334**, 195–200 (2011).
9. S. W. Huang, G. Cirmi, J. Moses, K. H. Hong, S. Bhardwaj, J. R. Birge, L. J. Chen, E. Li, B. J. Eggleton, G. Cerullo, and F. X. Kärtner, "High-energy pulse synthesis with sub-cycle waveform control for strong-field physics," Nature Photon. **5**, 475–479 (2011).
10. M. T. Hassan, Wirth, I. Grguraš, Moulet, T. T. Luu, J. Gagnon, V. Pervak, and E. Goulielmakis, "Invited article: attosecond photonics: synthesis and control of light transients." Rev. Sci. Instrum. **83**, 111301 (2012).
11. W. S. Warren, H. Rabitz, and M. Dahleh, "Coherent control of quantum dynamics: the dream is alive," Science **259**, 1581–1589 (1993).
12. G. Gademann, F. Plé, P. M. Paul, and M. J. J. Vrakking, "Carrier-envelope phase stabilization of a terawatt level chirped pulse amplifier for generation of intense isolated attosecond pulses," Opt. Express **19**, 24922–24932 (2011).
13. J. F. Hergott, O. Tcherbakoff, P. M. Paul, P. Demengeot, M. Perdrix, F. Lepetit, D. Garzella, D. Guillaumet, M. Comte, P. D. Oliveira, and O. Gobert, "Carrier-envelope phase stabilization of a 20 w, grating based, chirped-pulse amplified laser, using electro-optic effect in a $LiNbO_3$ crystal," Opt. Express **19**, 19935–19941 (2011).
14. A. V. Sokolov, M. Y. Shverdin, D. R. Walker, D. D. Yavuz , A. M. Burzo, G. Y. Yin, and S. E. Harris, "Generation and control of femtosecond pulses by molecular modulation," J. Mod. Opt. **52**, 285–304 (2005).
15. A. Burzo, A. Chugreev, and A. Sokolov, "Optimized control of generation of few cycle pulses by molecular modulation," Opt. Commun. **264**, 454–462 (2006).
16. J. L. Krause, K. J. Schafer, and K. C. Kulander, "High-order harmonic generation from atoms and ions in the high intensity regime," Phys. Rev. Lett. **68**, 3535–3538 (1992).
17. P. B. Corkum, "Plasma perspective on strong field multiphoton ionization," Phys. Rev. Lett. **71**, 1994–1997 (1993).
18. P. M. Paul, E. S. Toma, P. Breger, G. Mullot, F. Augé, P. Balcou, H. G. Muller, and P. Agostini, "Observation of a train of attosecond pulses from high harmonic generation," Science **292**, 1689–1692 (2001).
19. G. Sansone, E. Benedetti, F. Calegari, C. Vozzi, L. Avaldi, R. Flammini, L. Poletto, P. Villoresi, C. Altucci, R. Velotta, S. Stagira, S. D. Silvestri, and M. Nisoli, "Isolated single-cycle attosecond pulses," Science **314**, 443–446 (2006).
20. E. Goulielmakis, M. Schultze, M. Hofstetter, V. S. Yakovlev, J. Gagnon, M. Uiberacker, A. L. Aquila, E. M. Gullikson, D. T. Attwood, R. Kienberger, F. Krausz, and U. Kleineberg, "Single-cycle nonlinear optics," Science **320**, 1614–1617 (2008).
21. K. Zhao, Q. Zhang, M. Chini, Y. Wu, X. Wang, and Z. Chang, "Tailoring a 67 attosecond pulse through advantageous phase-mismatch," Opt. Lett. **37**, 3891–3893 (2012).
22. D. E. Spence, P. N. Kean, and W. Sibbett, "60-fsec pulse generation from a self-mode-locked ti: sapphire laser," Opt. Lett. **16**, 42–44 (1991).
23. C. Li, E. Moon, and Z. Chang, "Carrier-envelope phase shift caused by variation of grating separation," Opt. Lett. **31**, 3113–3115 (2006).
24. Z. Chang, "Carrier-envelope phase shift caused by grating-based stretchers and compressors," Appl. Opt. **45**, 8350–8353 (2006).
25. M. Kakehata, H. Takada, Y. Kobayashi, K. Torizuka, Y. Fujihira, T. Homma, and H. Takahashi, "Single-shot measurement of carrier-envelope phase changes by spectral interferometry," Opt. Lett. **26**, 1436–1438 (2001).
26. F. Lücking, V. Crozatier, N. Forget, A. Assion, and F. Krausz, "Approaching the limits of carrier-envelope phase stability in a millijoule-class amplifier." Opt. Lett. **39**, 3884–7 (2014).
27. A. Baltuška, T. Fuji, and T. Kobayashi, "Controlling the carrier-envelope phase of ultrashort light pulses with optical parametric amplifiers," Phys. Rev. Lett. **88**, 133901 (2002).
28. W. A. Okell, T. Witting, D. Fabris, D. Austin, M. Bocoum, F. Frank, A. Ricci, A. Jullien, D. Walke, J. P. Marangos, L. M. Rodrigo, and J. W. G. Tisch, "Carrier-envelope phase stability of hollow fibers used for high-energy few-cycle pulse generation," Opt. Lett. **38**, 3918–3921 (2013).
29. B. E. Schmidt, A. D. Shiner, M. Giguère, P. Lassonde, C. H. Trallero, J. C. Kieffer, P. B. Corkum, D. M. Villeneuve, and F. Légaré, "High harmonic generation with long-wavelength few-cycle laser pulses," J. Phys. B **45**, 074008 (2012).
30. S. W. Huang, G. Cirmi, J. Moses, K. H. Hong, S. Bhardwaj, J. R. Birge, L. J. Chen, I. V. Kabakova, E. Li, B. J.

Eggleton, G. Cerullo, and F. X. Kärtner, "Optical waveform synthesizer and its application to high-harmonic generation," J. Phys. B **45**, 074009 (2012).
31. T. Rathje, N. G. Johnson, M. Möller, F. Süß mann, D. Adolph, M. Kübel, R. Kienberger, M. F. Kling, G. G. Paulus, and a. M. Sayler, "Review of attosecond resolved measurement and control via carrierenvelope phase tagging with above-threshold ionization," J. Phys. B **45**, 074003 (2012).
32. T. Wittmann, B. Horvath, W. Helml, M. G. Schätzel, X. Gu, A. L. Cavalieri, G. G. Paulus, and R. Kienberger, "Single-shot carrier-envelope phase measurement of few-cycle laser pulses," Nature Phys. **5**, 357–362 (2009).

1. Introduction

Since the invention of femtosecond (fs) Ti:Sapphire lasers, much effort has been put into the pursuit of shorter and more energetic laser pulses with an ultimate goal of measuring, studying and controlling electronic dynamics, which naturally occur on the attosecond time scale [1]. Seminal work in the last two decades boosted pulse energies to milijoule (mJ) or even joule level while achieving pulse durations as short as a few fs. The former was achieved using the chirped-pulse-amplification (CPA) technique [2], and the latter was realized through nonlinear optical processes such as self-phase-modulation (SPM) in a gas filled hollow-core fiber (HCF) [3] or via filamentation [4]. Owing to development in both areas, terawatt [5], or even petawatt [6] class lasers are now available. However, further accessing even shorter, sub-cycle, pulse durations in the optical regime with a high energy has been quite challenging due to experimental difficulties in coherently generating multi-octave bandwidths, as well as compensating for the resulting dispersion. Recently, the technique of synthesizing laser pulses covering different spectral regions [7, 8, 9, 10] has shown promise path for generating energetic sub-cycle laser pulses. This technique also provides the ability to tailor sub-cycle waveforms for potential applications such as arbitrary waveform generation [10], quantum control [11], etc. Nevertheless, the key ingredient for a light field synthesizer—a carrier-envelope-phase (CEP) stable laser system—has been technically challenging and, so far, mostly restricted to systems with a few mJ energy, thus limiting the synthesized pulse energy to the μJ level [8, 9]. To date, only a few CEP stable lasers with tens of mJ have been reported with < 300 mrad single-shot CEP stability [12, 13]. It should be mentioned that another competing technique for generating ultrabroadband pulses, using Raman sidebands, also suffers from a limitation on the maximum achievable energy per pulse [14, 15].

Accessing even shorter time scales requires the use of high-harmonic generation (HHG) [16, 17], which has enabled laser pulses in the extreme ultraviolet (XUV) region with attosecond pulse durations. Attosecond pulses can be created as part of an attosecond pulse train (APT) [18] or as isolated attosecond pulses (IAPs) [19], depending on the number of electron collisions with the parent atom. Since HHG is intrinsically a sub-cycle phenomenon, it is ideal to have a sub-cycle laser field to enable the generation of IAPs. However, due to the lack of laser sources that provide sub-cycle pulses, IAPs are often generated by using ionization gating to select part of the XUV spectrum driven by a CEP stable few-cycle laser [20] or by using optical gating to reduce the number of collisions in a CEP stable few-cycle or multi-cycle laser [21]. Both methods sacrifice either the usable XUV energy or the driving laser energy, thus limiting the generated IAPs to nJ energies or smaller.

It is intuitive to link the inefficient use of energy of the two methods. Both point to the need for a CEP stable high energy laser source. In this paper, we present our achievement of a CEP stable, terawatt level, Ti:Sapphire laser system, which is a vital first step towards generating energetic, synthesized, sub-cycle laser pulses and the creation of more energetic IAPs. We start with a detailed description of the construction of the laser, then focus on a critical part of this realization —vibrational damping of the stretcher and compressor. We then present the resulting single-shot CEP noise values of 250 mrad over 1 hour and 300 mrad over 9 hours. Also, we briefly discuss the use of this laser source to pump an optical parametric amplifier (OPA) as

#231111 - $15.00 USD Received 29 Dec 2014; accepted 2 Feb 2015; published 12 Feb 2015

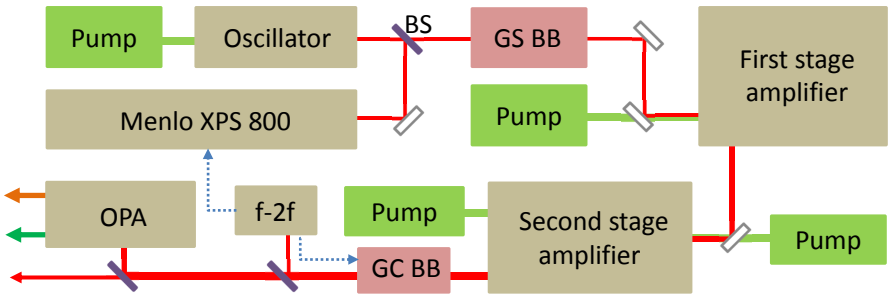

Fig. 1. Layout of the 1 kHz, 20 mJ, 26 fs laser system. BS: beam splitter; GS BB: grating stretcher breadboard; GC BB: grating compressor breadboard. See text for design details.

well as the possibilities of generating mJ level sub-cycle pulses.

2. A 1 kHz, 20 mJ, 26 fs Ti:sapphire laser system

A schematic of the laser system is shown in Fig. 1.The oscillator operates at 78 MHz and consists of the traditional soft-aperture Kerr lens modelocking design [22], utilizing a prism pair for intracavity dispersion compensation. The oscillator is pumped by a frequency doubled diode-pumped-solid-state (DPSS) laser (Lighthouse Sprout G). A portion of the oscillator output is used to stabilize the oscillator CEP with a Menlo Systems XPS800 f-2f interferometer with the SYNCRO electronics package. The CEP noise correction is provided by moving the high reflector in the dispersed arm of the oscillator. Every fourth pulse of the resulting pulse train typically carries CEP noise of 110 mrad in the integration range from 1 Hz to 2 MHz. In order to make the system more stable, the pump laser, oscillator, and the XPS800 are integrated into a single box.

The output of the oscillator, or seed laser, passes through two Faraday rotators to prevent back propagation of the seed or amplified light into the oscillator. The seed then propagates into a grating-based stretcher and is stretched to around 200 ps for CPA. Since the CEP noise accumulated in the amplification stages mainly originates from the stretcher and compressor [23, 24], both are mounted on separate breadboards for noise reduction (discussed in section 3). The seed laser out of the stretcher is sent to a Pockels cell, in which a 1 kHz pulse train is picked off and sent to the first multipass amplification stage. The first stage consists of a total of fourteen passes in a ”ring” amplifier. The gain medium is a Brewster cut Ti:Sapphire crystal optically pumped by a frequency doubled, 35 W, Q-switched, DPSS pump laser (Photonics Industries DM35). The first six passes go through a gain flattening filter to reduce gain around the center wavelength (∼790nm). Upon amplification this configuration produces a super Gaussian output spectrum with a FWHM in excess of 60 nm and tail to tail width of 120 nm. The crystal is cooled to below -200°C with a cold helium cryogenic cooling system (CryoMech) to avoid thermal lensing. The first amplification stage produces a 1 kHz, 2 mJ pulse train which is then sent to a second Pockels cell to attenuate pre/post-pulses and amplified spontaneous emission. The second amplification stage consists of a five-pass amplifier in a “bow tie” configuration optically pumped by two frequency doubled, 50 W, Q-switched, DPSS pump lasers (Photonics Industries DM50). The gain medium is a normal cut Ti:Sapphire crystal rod with anti-reflection coatings on both ends. The crystal is cooled by the same cooling system used in the first stage crystal. The mode size of the seed laser and the pump lasers is carefully matched to increase the efficiency of the amplification (∼30%), resulting in a 1 kHz, 29 mJ output. The size of the laser beam is expanded to about 3 cm in diameter ($1/e^2$) before being sent to the grating-based

#231111 - $15.00 USD Received 29 Dec 2014; accepted 2 Feb 2015; published 12 Feb 2015

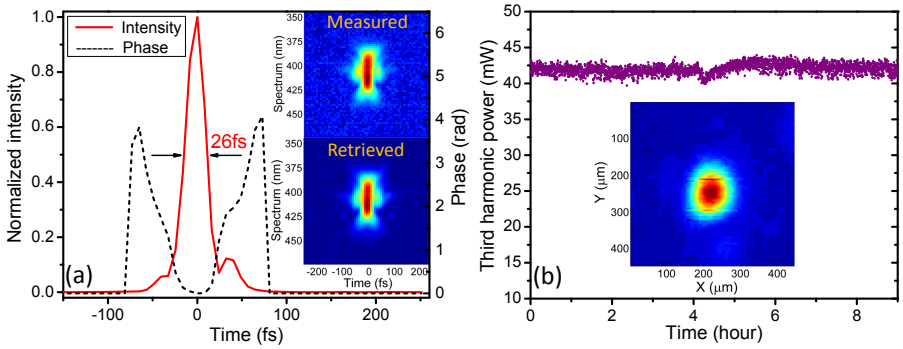

Fig. 2. (a) The retrieved laser electric field amplitude and the temporal phase as measured by SHG FROG. The measured and retrieved FROG traces are plotted in the inset. (b) The power stability measurement of the third harmonic power of the laser output for 9 hours. The inset shows the focus of the laser using a 3m lens.

compressor. An overall transmission efficiency of ∼70% is achieved through the compressor and gives a 1 kHz, 20 mJ, 26 fs output. A second-harmonic frequency-resolved optical gating (SHG FROG) measurement is shown in Fig. 2(a) to indicate the achieved pulse duration. To interrogate the stability of the laser pulse energy, the power of the third harmonic of the amplifier output was measured for 9 hours, resulting in a standard deviation of 1.6%, as shown in Fig. 2(b). The focused beam profile is also shown in the inset of Fig. 2(b) with an M^2 value of 1.36 along the X axis and 1.27 along the Y axis.

The CEP noise accumulated in the CPA process is measured by a sapphire crystal based f-2f interferometer [25]. A portion of the interferometric signal is split off for single-shot spectral fringe detection using a spectrometer with 1 ms integration time. The rest is sent to a quadrant position sensitive photodiode to measure the “jitter” of a single-shot fringe pattern. The photodiode signal is integrated to give an analog error signal with a bandwidth up to the repetition rate of the amplifier, in this case, 1 kHz. This analog error signal is then processed in a proportional-integral-derivative (PID) controller and used as feedback to both the oscillator and compressor gratings. The feedback to the oscillator is termed fast-loop. It pre-compensates the fast drifts of the CEP by modulating the same high reflector used for oscillator CEP locking. The feedback to the compressor grating is termed slow-loop. It drives the piezo stage under one of the gratings using a PID program to correct for long-term CEP drifts. The effect of the initial vibration mitigation technique on amplifier CEP stability is shown in Fig. 3(a) with a single-shot CEP error of 880 mrad, which was impractically large for our purposes. Note that the cryogenic cooling system is located in a separate room to reduce vibrations. Also, both the stretcher and compressor sub-breadboards were mounted with a vibration absorbing mat (Rathburn Associates ISODAMP C-1000) underneath to reduce vibrational energy transmitted through the optical table. The sub-breadboards were secured to the amplifier breadboard with vertical clamps. A more effective vibrational damping method was needed in order to reduce the CEP error as described below.

3. Improved vibrational damping of the stretcher and compressor and CEP results

A modified vibrational damping method is sketched in Fig. 4(a). Four rubber bushings were installed underneath each breadboard (the rubber bushings are squeezed severely in practice) to reduce contact of the breadboard with the optical table. Lateral and vertical clamps are used to ”squeeze” the breadboard in place instead of using bolts. The clamps were found to transmit less

#231111 - $15.00 USD Received 29 Dec 2014; accepted 2 Feb 2015; published 12 Feb 2015

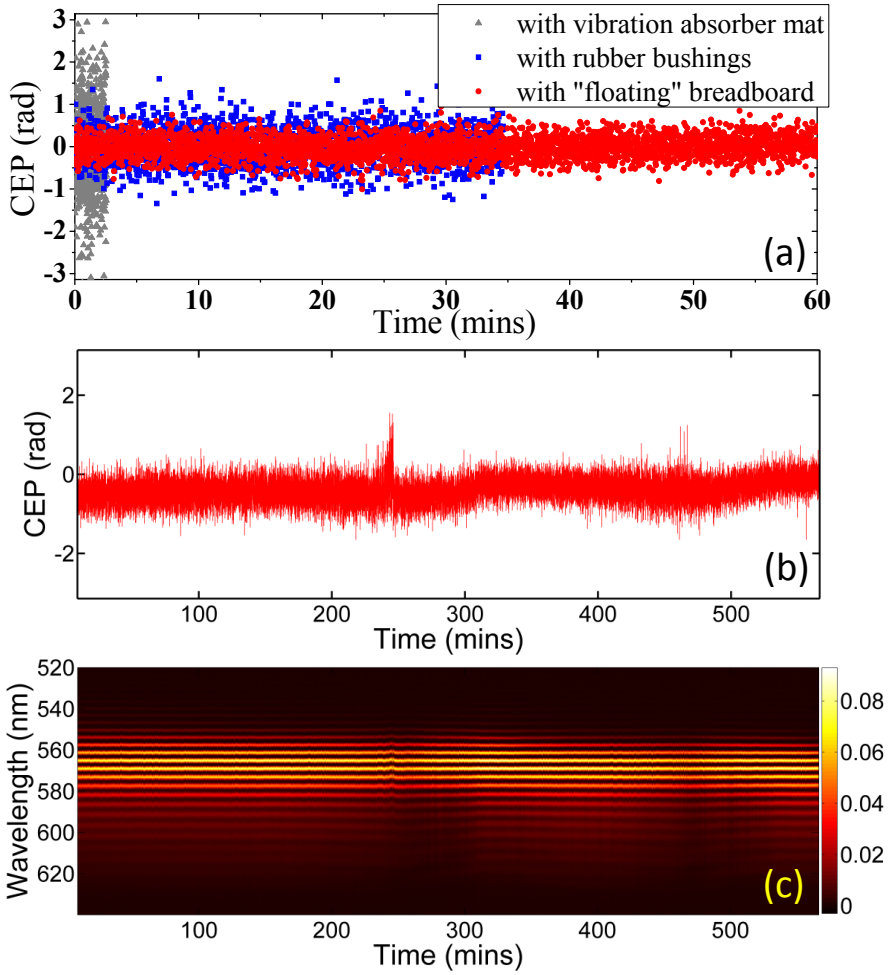

Fig. 3. (a) Short-term single-shot CEP error as measured in the three different vibrational damping schemes. (b) Long-term single shot CEP error with the “floated” stretcher and compressor. (c) The spectral fringes for the long-term CEP stabilization using the floating and compressor and stretcher. All measurements performed with an f-2f interferometer.

#231111 - $15.00 USD
Received 29 Dec 2014; accepted 2 Feb 2015; published 12 Feb 2015

vibrational energy from the optical table to the sub-breadboard. In this design, the breadboard is less susceptible to lateral and vertical vibrational energy transfer than in the initial design. The vibrational frequencies present on the breadboard were measured with an accelerometer and characterized with a vector signal analyzer. The results with the vibration absorber mat and the rubber bushings are compared in Fig. 4(c). Considerable reduction of vibrational frequencies above 50 Hz is achieved with the new damping method, although the 30 Hz noise is enhanced by almost a factor of 2 compared to the absorbing mat, and the 60 Hz noise remains prominent. The CEP noise in this case was measured to have single-shot error of 425 mrad, as shown in Fig. 3(a). This was more than a two-fold improvement of the CEP stability over the initial design. One of the main drawbacks of this mounting scheme is that since the breadboard is less constrained, it takes much longer for the laser pointing out of the stretcher and compressor to be stabilized and the whole system is more sensitive to room temperature fluctuations. Note that, in our case, the laser room temperature is controlled to within ± 1 °C, making the effect of the temperature fluctuation not as significant.

To further enhance the CEP stability, the vibrational energies at 30 and 60 Hz needed to be attenuated. This was achieved by "floating" both breadboards. This floating scheme is different from optical table floating, in which high pressure air is used to push the optical table above the supporting legs. In our case, a special mount is utilized as sketched in Fig. 4(b). It includes two parts. The first is bolted on the optical table and has a container for a thick piece of polyurethane (Sorbothane®). The second part is bolted to the breadboard and has a bolt threaded through one side. This bolt is coupled to a movable rod which sits on the polyurethane cylinder held by the first part. Four of these mounts are placed at the corner of each breadboard. By tightening the bolt above the removable rod, the breadboard can be lifted off the optical table and carefully balanced and leveled. The force of the breadboard pushing onto the polyurethane pieces produces a cone shaped pocket around each rod. These cones allow for lateral constraint of the breadboard while still maintaining isolation from the table itself. The only way that any vibrational energy from the table can couple into the breadboard is through the polyurethane piece and the rod. Using this mounting method the breadboards for both the stretcher and compressor, vibrations are significantly attenuated compared to the previous mounting schemes, as illustrated in Fig. 4(c). The 30 and 60 Hz vibrational energies and the overall vibrations below 100 Hz are attenuated significantly. Under this condition, the single-shot CEP variation is locked within 250 mrad for an hour as shown in Fig. 3(a). Since the breadboards are much less constrained in this case, it takes a few days for the polyurethane pieces and the breadboards to reach equilibrium. An overnight CEP locking was performed after the system was stabilized and resulted in a 300 mrad single-shot CEP error over a 9 hour period. To the best of our knowledge, these values are among the best short- and long-term CEP noise values reported for a terawatt class laser system. The result is shown in Fig. 3(b) along with the spectral fringe pattern (Fig. 3(c)). The spike around 250 minutes occurred when the fast-loop PID reached the locking limit, but it was driven back by the slow-loop. A temperature fluctuation caused the slightly dimmer spectral fringe at around 300 and 500 minutes, but did not seem to affect the CEP locking.

Recently, a CEP stabilized amplifier system producing 0.8 mJ of energy per 25 fs pulse at 10 kHz was reported [26]. The phase noise for this amplifier was reported to be 98 mrad measured in-loop and 140 mrad measured out-of-loop for periods of 50 s. While similar methodology (separate high and low frequency feedback) for active phase stabilization was used in that amplifier more attention was needed to address the mechanical sources of phase noise stemming from the reflection grating based stretcher and compressor. In order to avoid optical component damage at pulse energies above 10 mJ it is more practical to use the grating approach for chirped pulse amplification. In addition, a ten-fold lower repetition rate is required to reach TW peak

#231111 - $15.00 USD Received 29 Dec 2014; accepted 2 Feb 2015; published 12 Feb 2015

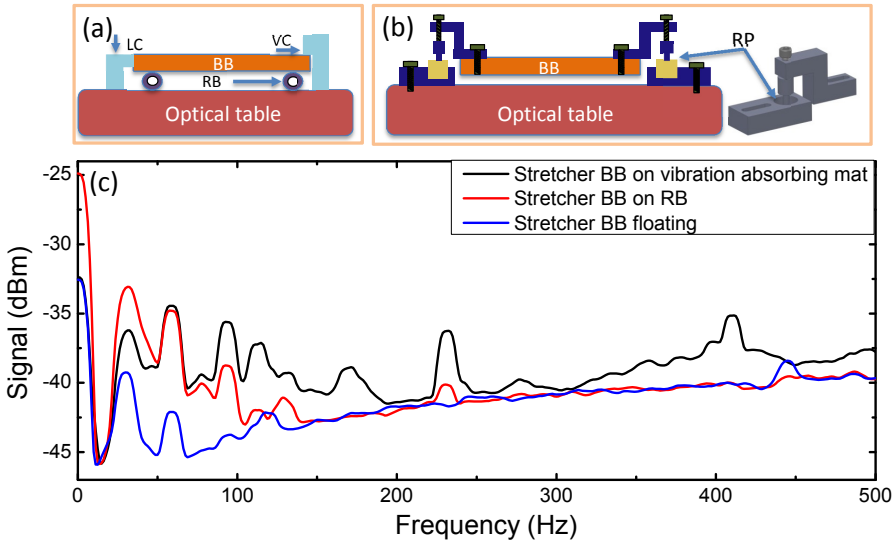

Fig. 4. (a) The mounting scheme for the vibrational damping method using rubber bushings. LC: lateral clamp; VC: vertical clamp; BB: breadboard; RB: rubber bushing (b) The mounting scheme for the vibrational damping method using "floating" breadboards. RP: rubber plug (c) The vibrational energy spectrum with three different methods, measured on the stretcher breadboard.

powers producing a ten-fold decrease in the available feedback bandwidth. This severe feedback bandwidth limitation further necessitates effective mechanical decoupling of the stretcher and compressor. Furthermore, production of IAPs and their ultimate experimental applications necessitates the use of vacuum pumping machinery that can couple vibrational energy into the laser amplifier system that will contribute to phase noise through the grating based stretcher and compressor. Finally, we should stress that the very impressive values of 98 mrad and 140 mrad in the CEP rms noise reported in [26] were only sustained for 50s. On the other hand, our goal was to make CEP control experimentally usable by extending the lock time to several hours.

4. Towards generation of mJ level sub-cycle synthesized laser pulses

Out of the 20 mJ of total energy, we split the laser output into two arms (see Fig. 1), one with 2 mJ pulse energy and the other with 18 mJ pulse energy. The 18 mJ arm pumps a white-light-seeded OPA system (Light Conversion HE-TOPAS-Prime-Plus). The OPA consists of three amplification stages. In the first stage, 1-3 μJ pulse energy is used for generating signal wavelength through SPM in a sapphire crystal. The generated signal beam is then preamplified by mixing it with $\sim$35 μJ of 800 nm light in a Type II β-barium borate (BBO) crystal. The second stage further enhances the signal energy to a level of about 100 μJ by pumping it with $\sim$700 μJ of 800 nm light in a second Type II BBO crystal. In the final stage, a $\sim$17.2 mJ pump laser boosts the total energy of the signal (S) and idler (I) to 6 mJ with a 60/40 S/I ratio when the signal is tuned to 1320 nm. By tuning the angle of the BBO crystals, the wavelength of the signal (idler) can be tuned from 1150 to 1600 nm (1600 to 2600nm). The achieved pulse energy at different wavelengths is shown in Fig. 5(b).

In order to have sub-cycle laser pulses, the 2 mJ pump beam (800 nm) and the 6 mJ S+I beam need to be spectrally broadened and then synthesized. This is a very similar procedure

#231111 - $15.00 USD Received 29 Dec 2014; accepted 2 Feb 2015; published 12 Feb 2015

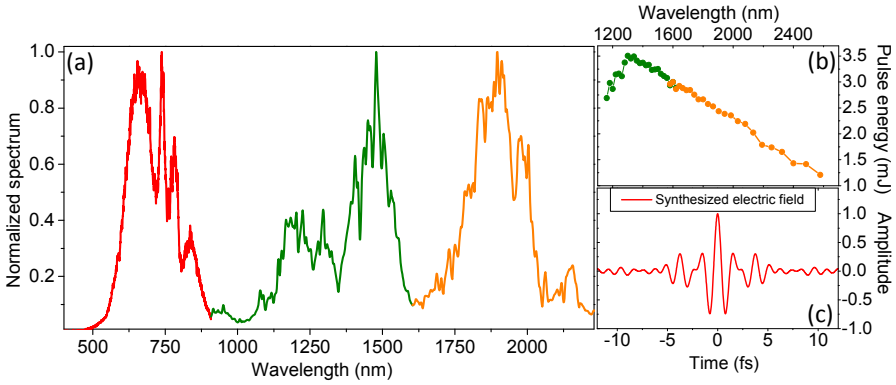

Fig. 5. (a) The broadened spectrum of pump, signal and idler. (b) OPA output energies as a function of wavelength. (c) Theoretically calculated synthesized electric field using spectrum from (a) and assuming a flat phase across the whole spectrum.

to that done in [8, 10]. Due to the fact that the SPM process preserves CEP, the signal output should ideally inherit the same CEP from the pump [27]. Any small CEP drifts can also be corrected by rotating a pair of glass plates in the OPA with a piezo motor. Furthermore, the idler output is known to have passive CEP stability [27], and spectral broadening in HCFs has also been shown to maintain CEP stability [28, 29]. Therefore, if the time separation of all three pulses can further be precisely stabilized and delayed [30], mJ level sub-cycle synthesized laser pulses could be realized. In our case, we were able to obtain more than 2.5 mJ of energy per pulse in the broadened pump, signal and idler. By adding all three broadened spectra, we obtain the multi-octave spectrum shown in Fig. 5(a). Both the energy per pulse and the broadening represent lower limits of what is possibly achievable, yet we have been able to achieve almost three octaves of bandwidth and multi-mJ energies. Such achievements emphasize the strength of our method. We need to point out that at this stage we haven't compressed the broadened pulses, nor recombined them. A theoretical calculation of the time-domain synthesized laser pulse is shown in Fig. 5 (c). This calculation is simply a Fourier transform of a transform limited pulse with the spectrum shown in Fig. 5 (a). The experiments for the compression and synthesis are in progress and will be reported in the future.

5. Concluding remarks

To conclude, we have demonstrated a 0.77 TW Ti:Sapphire laser system that is CEP stable for extended periods of time. The laser delivers 20 mJ, 26 fs pulses at 1 kHz repetition rate with center wavelength of 790 nm. We measured CEP single-shot RMS noise of 250 mrad over one hour and 300 mrad over 9 hours. In our opinion these measurements represent some of the best CEP noise levels for a terawatt class laser. Our emphasis is on the long-term stability of very intense laser pulses. The low CEP RMS noise obtained by us, over such long times, makes CEP-controlled experiments, with intense fs pulses, a possibility. Such research is still considered quite challenging and is mostly performed in a CEP tagged fashion [31, 32]. To achieve such low noise, we developed a new mounting scheme, in which both stretcher and compressor are "floating" and, therefore, isolated from vibrational noise on the optical table. The noise sources and frequencies were obtained by Fourier analysis of the f-2f feedback signal and the mounts were tuned to mitigate such frequencies. With this approach the resulting short- and long-term CEP stabilities are both significantly improved. We are currently exploring better vibrational damping methods to further improve CEP stability. With the excellent short- and

#231111 - $15.00 USD Received 29 Dec 2014; accepted 2 Feb 2015; published 12 Feb 2015

long-term CEP stabilities at such high energy and repetition rate, stable and energetic ($>$ 2 mJ energy per pulse) sub-cycle laser pulses are feasible by synthesizing spectrally-broadened fundamental and OPA outputs. Energetic optical synthesis promises generation of high energy per pulse, high flux (1 kHz repetition rate), and high photon-energy XUV sources and opens a new door towards the generation of bright isolated attosecond pulses and strong field coherent control.

Acknowledgments

The HITS laser was mainly financed by NSF-MRI grant No:1229672, with additional contributions from DOD-DURIP grant No. FA2386-12-1-3014 and DOE grant No. DE-FG02-86ER13491. Operational cost of the laser as well as support for CAT-H, VK, IB-I, KDC, DJW, AMS, and SZ was provided by the Chemical Sciences, Geosciences, and Biosciences Division, Office of Basic Energy Sciences, Office of Science, U.S. Department of Energy (DOE) under Grant No. DE-FG02-86ER13491. DJW was partially supported by the National Science Foundation Graduate Research Fellowship under Grant No. DGE-1247193. AMS was partially supported by the Department of Defense (DoD) through the National Defense Science & Engineering Graduate Fellowship (NDSEG) Program. XR was supported by NSF-MRI grant No:1229672. Finally, we would like to acknowledge that the long-term CEP stability was made possible by the environmentally stable lab space recently upgraded by Kansas State University.

#231111 - $15.00 USD Received 29 Dec 2014; accepted 2 Feb 2015; published 12 Feb 2015